

## Single-Crystal Reflectance Studies of Tetrathiafulvalene Tetracyanoquinodimethane\*

C. S. Jacobsen,† D. B. Tanner,‡ A. F. Garito, and A. J. Heeger  
*Department of Physics and Laboratory for Research on the Structure of Matter,  
 University of Pennsylvania, Philadelphia, Pennsylvania 19174*

(Received 14 October 1974)

The polarized reflectance of single crystals of tetrathiafulvalene tetracyanoquinodimethane (TTF-TCNQ) at 300 K is reported over the frequency range 300 to 4000  $\text{cm}^{-1}$ , with unpolarized data extending to 50  $\text{cm}^{-1}$ . A Kramers-Kronig analysis is used to obtain the frequency-dependent conductivity  $\sigma_1(\omega)$  and dielectric function,  $\epsilon_1(\omega)$ , for both  $a$  and  $b$  crystallographic axes. The results establish the existence of the energy gap and provide a quantitative measurement of the oscillator strength and relaxation time of the collective mode.

The existence of a gap<sup>1</sup> in the electronic excitation spectrum of tetrathiafulvalene-tetracyanoquinodimethane (TTF-TCNQ) is of central importance to understanding the origin of the remarkable transport properties of this organic metal.<sup>2-6</sup> The energy gap in the infrared ( $E_g \approx 0.14$  eV) together with the relatively large dc<sup>2-4</sup> and microwave<sup>6</sup> conductivities imply a correlated many-body state in which the low-frequency conductivity results from a collective mode. We report single-crystal reflectivity measurements in the range from 50 through 4000  $\text{cm}^{-1}$ . The results confirm the energy gap as obtained from earlier work on thin films,<sup>1</sup> and place a lower limit on the collective-mode lifetime.

The infrared (ir) reflectivity measurements were performed on single crystals ca.  $2 \times 10$  mm<sup>2</sup> using as-grown surfaces.<sup>7</sup> ir spectra were recorded using a Perkin-Elmer 225 spectrophotometer over the region 300 to 4000  $\text{cm}^{-1}$ , and a Grubb-Parsons Michelson interferometer in the range from 50 to 500  $\text{cm}^{-1}$ . Figure 1 shows the polarized reflectance at room temperature for  $E \parallel b$  and  $E \parallel a$  in the range 300–4000  $\text{cm}^{-1}$ . The dashed lines from 50 to 300  $\text{cm}^{-1}$  were obtained from unpolarized reflectance from carefully aligned single crystals;  $R(E \parallel b)$  was calculated by assuming that  $R(E \parallel a)$  is constant at the 300- $\text{cm}^{-1}$  value, so that  $R(E \parallel b) = 2R_{\text{unpolarized}} - R(E \parallel a)$ . Throughout the ir,  $R(E \parallel a)$  is essentially frequency independent except for several sharp structures arising from intramolecular vibrations.

Over the intermediate ir,  $R(E \parallel b)$  has values of less than 72%, i.e., considerably below the values that would be expected from a simple metal with a dc conductivity<sup>2-4</sup> between 500–1000 ( $\Omega \text{ cm}$ )<sup>-1</sup> and a plasma edge at 7000  $\text{cm}^{-1}$ .<sup>8-11</sup> The relatively low reflectance at long wavelengths implies an energy gap  $E_g = \hbar\omega_g$  with  $\omega_g\tau_{sp} \sim 1$ ,

where  $\tau_{sp}$  is the single-particle scattering time appropriate to excitations near the gap edge.

Since the polarized reflectance is known for frequencies up to 37000  $\text{cm}^{-1}$ ,<sup>8-10</sup> a Kramers-Kronig analysis is expected to give reliable results in the ir. This procedure consists of calculating the phase shift  $\theta(\omega)$  from the dispersion relation:

$$\theta(\omega) = \frac{\omega}{\pi} P \int_0^{\infty} \frac{\ln R(\omega') - \ln R(\omega)}{\omega^2 - \omega'^2} d\omega'. \quad (1)$$

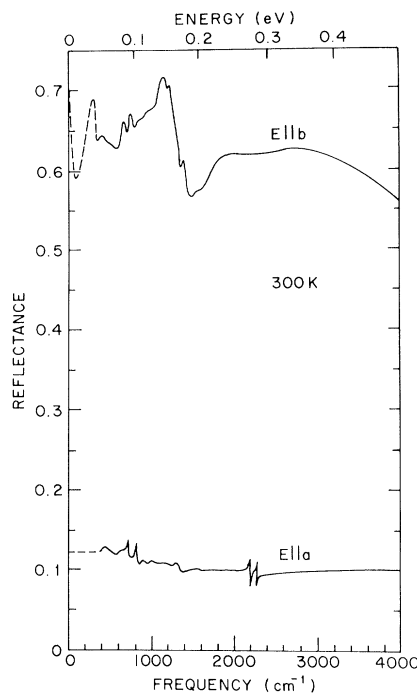


FIG. 1. Single-crystal reflectance of TTF-TCNQ. The curves labeled  $E \parallel b$  and  $E \parallel a$  represent polarized reflectance data with electric field vector parallel to the crystallographic  $b$  and  $a$  axes, respectively.

The complex index of refraction is then obtained from the inverted Fresnel formula

$$N = n + ik = [\epsilon_1 + i(4\pi/\omega)\sigma_1]^{1/2} \\ = (1 + R^{1/2}e^{i\theta}) / (1 - R^{1/2}e^{i\theta}). \quad (2)$$

Since  $R(\omega)$  is known for  $50 < \omega < 37\,000 \text{ cm}^{-1}$ , conventional extrapolation procedures were employed.<sup>12</sup> In the range  $0 < \omega < 50 \text{ cm}^{-1}$ , it was assumed that  $R(E \parallel b)$  behaves according to the Hagen-Rubens formula,  $R = 1 - A\omega^{1/2}$ , with the parameter  $A$  chosen so that a smooth connection with the data was obtained. The value for  $R(E \parallel a)$  was assumed constant in this range. The high-frequency extrapolation must simulate interband and (at very high frequencies) free-electron behavior. For the  $b$ -axis data we have used the standard approximation,  $R(\omega) = R(\omega_c)(\omega_c/\omega)^P$ , with  $\omega_{c1} = 37\,000 \text{ cm}^{-1}$ ,  $P_1 = 2$  (corresponding to interband transitions), and with  $\omega_{c2} = 2 \times 10^5 \text{ cm}^{-1}$ ,  $P_2 = 4$  (corresponding to free-electron behavior).

The frequency-dependent conductivity  $\sigma_1(\omega)$  and dielectric function  $\epsilon_1(\omega)$ , as obtained from the Kramers-Kronig analysis, are shown for  $E \parallel b$  and  $E \parallel a$  in Figs. 2 and 3.

The insensitivity to the extrapolation procedures is illustrated by the following examples.

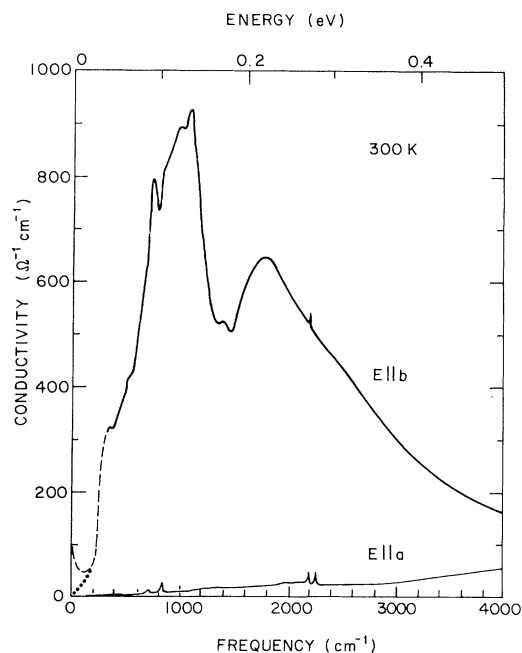


FIG. 2. The frequency-dependent conductivities  $\sigma_1^b(\omega)$  and  $\sigma_1^a(\omega)$  as obtained from Kramers-Kronig analysis. The dotted and dashed curves below  $200 \text{ cm}^{-1}$  represent two different low-frequency extrapolations (see text).

Assuming  $R(E \parallel b)$  constant for  $\omega < 50 \text{ cm}^{-1}$  leads to changes in  $\sigma_1$  less than 2% for  $\omega > 500 \text{ cm}^{-1}$ , and gives in the gap region even lower values for  $\sigma_1$  (the dotted curve below  $200 \text{ cm}^{-1}$ ) than the Hagen-Rubens extrapolation (the dashed curve below  $200 \text{ cm}^{-1}$ ). Assuming constant reflectance above  $37\,000 \text{ cm}^{-1}$  changes  $\sigma_1^b(\omega)$  less than 10% for any  $\omega < 10^4 \text{ cm}^{-1}$ , and has negligible effect below  $500 \text{ cm}^{-1}$ .

The main features in  $\sigma_1^b(\omega)$  are a resonant structure with an absolute maximum at approximately  $1100 \text{ cm}^{-1}$  with a relatively narrow minimum centered at approximately  $1400 \text{ cm}^{-1}$ . At higher frequencies a smooth, Drude-like frequency dependence is observed. The general shape and detailed structure are in excellent agreement with the thin-film data.<sup>1</sup> The larger peak value and narrower width of the single-crystal  $\sigma_1^b(\omega)$  imply a longer single-particle scattering time, as expected.<sup>8,9</sup>

The corresponding behavior of  $\epsilon_1^b(\omega)$  (Fig. 3) is that of an insulator with a transition across the energy gap sufficiently strong to give negative values between  $1000$  and  $6000 \text{ cm}^{-1}$ . At lower frequencies,  $\epsilon_1^b$  is positive with a maximum of 82 near  $300 \text{ cm}^{-1}$ , while the detailed behavior in the far ir is not known. The general shape

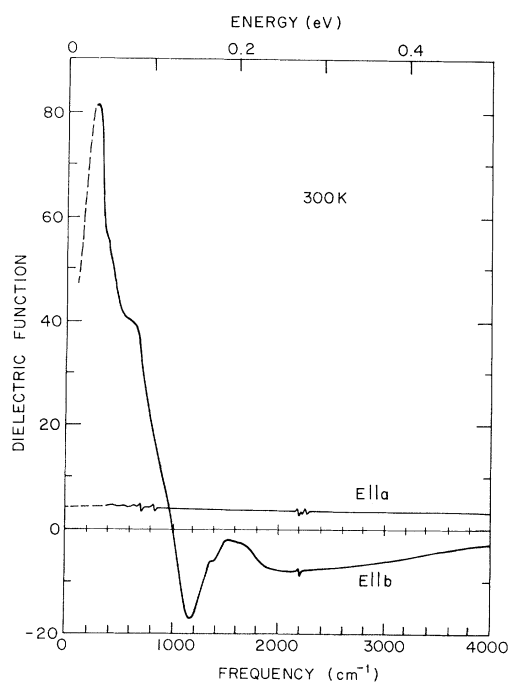


FIG. 3. The frequency-dependent dielectric functions  $\epsilon_1^b(\omega)$  and  $\epsilon_1^a(\omega)$  as obtained from Kramers-Kronig analysis.

and detailed structure are once again in excellent agreement with the thin-film data.<sup>1</sup>

The single-crystal reflectivity results thus establish the existence of the energy gap in the excitation spectrum. The gap is well defined even at room temperature where fluctuation effects would suggest a relatively high density of states in the gap region.<sup>13</sup> That there are states in the gap can be inferred from the magnetic susceptibility.<sup>14-16</sup> The susceptibility shows the qualitative features predicted by Lee, Rice, and Anderson,<sup>13</sup> and would imply that at room temperature the density of states near  $E_F$  is within 20% of the unperturbed value. In contrast,  $\sigma_1^b(\omega)$  in the gap region below  $400 \text{ cm}^{-1}$  is more than an order of magnitude below the gapless Drude curve. We infer that the pseudogap in  $\sigma_1(\omega)$  is in essence a mobility gap<sup>17</sup> caused by the strong dynamic fluctuations in local potential due to the inherent fluctuations in the one-dimensional system.

The *single-crystal* results for the frequency-dependent  $b$ -axis conductivity can thus be summarized as follows: (i) Zero frequency (dc): The conductivity is approximately  $10^3 (\Omega \text{ cm})^{-1}$  at room temperature, increasing to values exceeding  $10^4$ – $10^5 (\Omega \text{ cm})^{-1}$  near 58 K.<sup>2-4</sup> (ii) Microwave frequency ( $10^{10}$  GHz): The conductivity is approximately  $10^3 (\Omega \text{ cm})^{-1}$  at room temperature, increasing to values exceeding  $10^4 (\Omega \text{ cm})^{-1}$  near 58 K.<sup>6</sup> At both dc and microwave frequencies it appears likely that the peak conductivities are defect limited. (iii) Infrared frequencies: There is an energy gap<sup>1</sup> with magnitude  $\hbar\omega_g \approx 0.14 \text{ eV}$  above which the single-particle conductivity is Drude-like with a plasma frequency<sup>8-11</sup> of  $\hbar\omega_p \approx 1.2 \text{ eV}$ .

These results are sketched in Fig. 4, which is drawn to describe qualitatively the frequency dependence of  $\sigma_1(\omega)$  near 60 K using typical values.

The collective-mode lifetime  $\tau_c$  has not yet been measured directly. However, this width can be estimated from the collective-mode oscillator strength  $\Omega_p^2$  and the measured dc conductivity, since<sup>18</sup>  $\sigma_{\text{collective}} = (4\pi)^{-1} \Omega_p^2 \tau_c$ . An upper limit to  $\Omega_p^2$  can be inferred from the single-crystal data. Since the width is less than the lowest measuring frequency,  $\epsilon_1 = 100 - \Omega_p^2/\omega^2$ .  $\Re(E \parallel b)$  remains nearly constant at approximately 70% and does not begin to rise toward unity even in the range 50 to  $100 \text{ cm}^{-1}$ . Thus, we can conservatively construct the inequality  $\Omega_p^2 < 10^6 \text{ cm}^{-2}$  [a rapid rise toward  $\Re(E \parallel b) \sim 1$  is required when  $\epsilon_1 < 0$ ]. Using  $\sigma_{\text{dc}}(300 \text{ K}) = 10^3 (\Omega \text{ cm})^{-1}$  leads to  $\tau_c^{-1}(300 \text{ K}) < 3 \times 10^{12} \text{ sec}^{-1}$  ( $16 \text{ cm}^{-1}$ ). Assuming

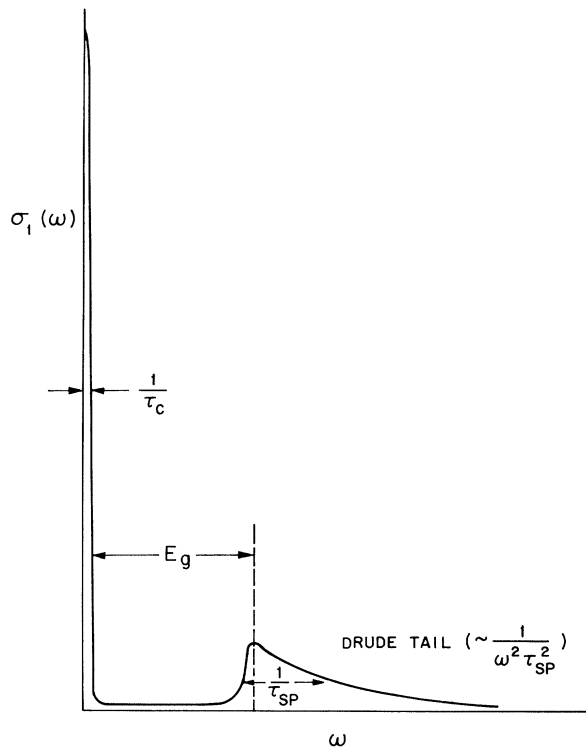


FIG. 4. Schematic diagram of  $\sigma_1^b(\omega)$  for TTF-TCNQ as obtained from single-crystal data (see text). The curve is drawn using a typical value of  $2 \times 10^4 (\Omega \text{ cm})^{-1}$  for the dc conductivity.

conservation of oscillator strength with decreasing temperature, a peak conductivity near 60 K in the range of  $10^4$ – $10^5 (\Omega \text{ cm})^{-1}$  implies  $\tau_c^{-1}(60 \text{ K}) \sim 10^{11} \text{ sec}^{-1}$  ( $\sim 0.5 \text{ cm}^{-1}$ ). Thus the collective-mode lifetime is enhanced over the single-particle scattering time by at least 2 orders of magnitude at room temperature and more than 3 orders of magnitude near 60 K. This comparison represents one of the clearest indications of coherence in the “metallic” state of TTF-TCNQ.

Much of the discussion surrounding the study of TTF-TCNQ and related systems centered on the dc electrical conductivity. However, it is now generally agreed that the intrinsic conductivity exceeds  $10^4 (\Omega \text{ cm})^{-1}$  and there is evidence that the peak value exceeds  $10^5 (\Omega \text{ cm})^{-1}$ .<sup>4</sup> The sensitivity of the one-dimensional conductor to impurities and defects has been established,<sup>4,6</sup> so that these values may only be lower bounds. However, it is most important to view the dc and microwave conductivities in the context of the overall experimental knowledge of  $\sigma_1(\omega)$  and  $\epsilon_1(\omega)$  as obtained from single-crystal data and the earlier work on thin films.<sup>1</sup> TTF-TCNQ is not a

simple metal; it has the optical spectrum of a semiconductor, but conducts at zero frequency because of a long-lifetime collective mode.

\*Work supported by the National Science Foundation through the Laboratory for Research on the Structure of Matter and Grant No. GH-39303, and by the Advanced Research Projects Agency through Grant No. DAHC 15-72C-0174.

†Present address: Physics Laboratorium III, The Technical University of Denmark, DK-2800 Lyngby, Denmark.

‡Present address: Physics Department, Ohio State University, Columbus, Ohio 43210.

<sup>1</sup>D. B. Tanner, C. S. Jacobsen, A. F. Garito, and A. J. Heeger, *Phys. Rev. Lett.* **32**, 1301 (1974).

<sup>2</sup>L. B. Coleman, M. J. Cohen, D. J. Sandman, F. G. Yamagishi, A. F. Garito, and A. J. Heeger, *Solid State Commun.* **12**, 1125 (1973).

<sup>3</sup>J. Ferraris, D. O. Cowan, V. Walatka, Jr., and J. H. Perlstein, *J. Amer. Chem. Soc.* **95**, 948 (1973).

<sup>4</sup>M. J. Cohen, L. B. Coleman, A. F. Garito, and A. J. Heeger, *Phys. Rev. B* **10**, 1298 (1974).

<sup>5</sup>P. M. Chaikin, J. F. Kwak, T. E. Jones, A. F. Garito, and A. J. Heeger, *Phys. Rev. Lett.* **31**, 601 (1973); J. F. Kwak, P. M. Chaikin, A. A. Russel, A. F. Garito, and A. J. Heeger, to be published.

<sup>6</sup>S. K. Khanna, E. Ehrenfreund, A. F. Garito, and A. J. Heeger, *Phys. Rev. B* **10**, 2205 (1974).

<sup>7</sup>These were all TTF-TCNQ(D<sub>8</sub>); the deuterated material grew into relatively large single crystals suitable for the infrared measurements.

<sup>8</sup>A. A. Bright, A. F. Garito, and A. J. Heeger, *Solid State Commun.* **13**, 943 (1974).

<sup>9</sup>A. A. Bright, A. F. Garito, and A. J. Heeger, *Phys. Rev. B* **10**, 1328 (1974).

<sup>10</sup>P. M. Grant, R. L. Greene, G. C. Wrighton, and G. Castro, *Phys. Rev. Lett.* **31**, 1311 (1973).

<sup>11</sup>P. I. Perov and J. Fischer, *Phys. Rev. Lett.* **33**, 521 (1974).

<sup>12</sup>See, for example, F. Wooten, *Optical Properties of Solids* (Academic, New York, 1972), p. 248.

<sup>13</sup>P. A. Lee, T. M. Rice, and P. W. Anderson, *Phys. Rev. Lett.* **31**, 462 (1973).

<sup>14</sup>J. C. Scott, A. F. Garito, and A. J. Heeger, *Phys. Rev. B* (to be published).

<sup>15</sup>J. H. Perlstein, J. P. Ferraris, V. V. Walatka, D. O. Cowan, and G. A. Candela, in *Magnetism and Magnetic Materials—1972*, AIP Conference Proceedings No. 10, edited by C. D. Graham, Jr., and J. J. Rhyne (American Institute of Physics, New York, 1973), p. 1494.

<sup>16</sup>Y. Tomkiewicz, B. A. Scott, L. J. Tao, and R. S. Title, *Phys. Rev. Lett.* **32**, 1363 (1974).

<sup>17</sup>A similar analysis leading to the inference of a mobility gap in K<sub>2</sub>[Pt(CN)<sub>4</sub>]Cl<sub>0.3</sub>·3H<sub>2</sub>O (KCP) has been presented by H. R. Zeller (private communication).

<sup>18</sup>M. J. Rice, S. Strässler, and W. R. Schneider, in "Saarbrücken Conference on One-Dimensional Conductors," Saarbrücken, Germany, June 1974, edited by H. G. Schuster (Springer, Berlin, to be published).

## From Giant Moment to Kondo and Spin Glass Behavior: The Electrical Resistivity of PdFe and (PdFe)H

J. A. Mydosh

*Institut für Festkörperforschung der Kernforschungsanlage, D-517 Jülich, Germany*  
(Received 1 October 1974)

I have measured the low-temperature electrical resistivity  $\rho(T)$  for a series of PdFe alloys with and without hydrogenation. For Pd+0.2 at.% Fe, the sharp decrease in  $\rho(T)$  at the Curie temperature gives way to a broad Kondo-like minimum. With increasing Fe concentration, the giant-moment ferromagnetism is severely hindered by hydrogen charging, and  $\rho(T)$  shows the characteristics of an interacting Kondo system or a "spin glass."

Palladium-iron is a well-known giant-moment system which orders ferromagnetically with small amounts of iron ( $c \approx 0.1$  at.% Fe).<sup>1-3</sup> On the other hand, elemental Pd can be easily charged with large amounts of hydrogen and becomes superconducting for H/Pd  $\approx 0.75$ .<sup>4,5</sup> It has further been established that the large exchange-enhanced Pauli paramagnetic susceptibility of Pd linearly decreases with hydrogenation, and at H/Pd  $\approx 0.65$  a slightly negative or diamagnetic susceptibility

is found.<sup>6</sup> Recent theories<sup>7,8</sup> have considered this result as a necessary (but not sufficient) condition for the rather high superconducting transition temperature ( $\approx 9$  K) of palladium hydride.<sup>5</sup>

As the exchange enhancement of Pd and the giant moments of PdFe lead to large effects in the electrical resistivity,<sup>9,10</sup> any modification of the Pd matrix polarizability should be strongly reflected in  $\rho(T)$  and  $d\rho(T)/dT$ . Furthermore, the hydrogenation of PdFe is especially signifi-